Hydrofluorination of Alkenes via Dual Co- and Photoredox Catalysis: Methodology Development and Electroanalytical Mechanistic Investigation

Jinjian Liu¹, Jian Rong², Devin P. Wood¹, Yi Wang¹, Steven H. Liang^{2*}, Song Lin^{1*}

¹Department of Chemistry and Chemical Biology, Cornell University, Ithaca, New York 14853, United States.

²Department of Radiology and Imaging Sciences, Emory University, Atlanta, Georgia 30322, United States.

ABSTRACT: The hydrofluorination of alkenes represents an attractive strategy for the synthesis of aliphatic fluorides. This approach provides a direct means to form C(sp³)–F bonds selectively from readily available alkenes. Nonetheless, conducting hydrofluorination using nucleophilic fluorine sources poses significant challenges due to the low acidity and high toxicity associated with HF and poor nucleophilicity of fluoride. In this study, we present a new Co(salen)-catalyzed hydrofluorination of simple alkenes, utilizing Et₃N·3HF as the sole source of both hydrogen and fluorine. This process operates via a polar-radical-polar crossover mechanism. We also demonstrated the versatility of this method by effectively converting a diverse array of simple and activated alkenes with varying degrees of substitution into hydrofluorinated products. Furthermore, we successfully applied this methodology to ¹8F-hydrofluorination reactions, enabling the introduction of ¹8F into potential radiopharmaceuticals. Our mechanistic investigations, conducted using rotating disk electrode voltammetry and DFT calculations, unveiled the involvement of both carbocation and Co¹V-alkyl species as viable intermediates during the fluorination step, and the contribution of each pathway depends on the structure of the starting alkene.

INTRODUCTION

The need to introduce fluorine atoms into organic molecules has increased dramatically in recent years in response to pharmaceutical and agrochemical needs. The unique properties of fluorine allow it to impart pertinent changes to the conformation, polarity, lipophilicity, and electrostatic properties of molecules, which can be leveraged for improved stability, potency, and bioavailability in biological settings.1 The percentage of fluorine-containing drug molecules among all pharmaceuticals is estimated to be 20% in recent years,2 and the broader incorporation of fluorine atom into drug design depends strongly on the availability of fluorination strategies. Because the half-life of 18F is favorable compared to alternative radioactive elements, ¹⁸Flabeled tracers are widely used in positron emission tomography (PET) for diseases diagnosis and drug discovery.3 Necessarily, methods to prepare fluorine-containing molecules are in high demand.

Hydrofluorination is a particularly appealing strategy to generate aliphatic fluorides because it offers a straightforward route to construct a $C(sp^3)$ –F bond in a regioselective fashion from olefins, one of the most abundant functionalities in organic molecules. However, direct hydrofluorination using HF is very challenging due to its low acidity and the poor nucleophilicity of F-. In addition, the high toxicity of gaseous HF also precludes its direct use in practical organic synthesis. To circumvent these issues, methods have been developed using electrophilic fluorine ([F+]) sources in combination with transition-metal hydrides (M-Hs) to hydrofluorinate alkenes (Scheme 1A). M-Hs can engage in

hydrogen-atom transfer (HAT) or hydrometallation with an alkene substrate to generate an alkyl radical or metal-bound alkyl complex, which can be subsequently fluorinated by an [F+] agent to deliver the desired product.⁴ Silanes and borohydrides are commonly employed as the terminal hydrogen-atom source to generate M–Hs in situ, wherein the formation of strong B–F and Si–F bonds provides the driving force for the formation of a weak and reactive M–H bond.⁵ Examples of electrophilic fluorinating reagents include selectfluor, *N*-fluorobenzenesulfonimide (NFSI), *N*-fluoropyridinium salts, and *N*-fluoro-*N*-aryl-sulfonamides. These fluorine sources usually also act as the oxidant to turn over the transition metal catalyst. ^{4,6}

Compared to electrophilic fluorine sources, nucleophilic fluorine ([F-]) agents are preferable from a cost and atom economy viewpoint. In addition, nucleophilic fluorination reactions can be directly amenable to 18F-fluorination reactions given that [18F]F-fluoride can be generated in large radioactivity from nuclear reaction ¹⁸O(p,n)¹⁸F by bombarding [180] H₂O and has substantially higher molar activity (A_m, A_m = radioactivity/mol) compared to electrophilic ¹⁸F sources generated from ¹⁸F₂.⁷ However, fluoride as a free anion is a strong base but a poor nucleophile, thus introducing selectivity issues wherein elimination competes with fluorination. Furthermore, the poor solubility of alkali fluoride salts makes them challenging to employ without phasetransfer or hydrogen-bonding mediators.8 Finally, F- is poorly compatible with silanes and borohydrides because of its high silica- and borophilicity, and as a result, its direct use in the aforementioned metal-hydride chemistry is difficult.

Although no general solutions are currently available for the nucleophilic hydrofluorination of simple alkenes, several seminal contributions have been made towards this objective (Scheme 1B).9 One strategy entails the complexation of gaseous HF with a Brønsted base to make a liquid or solid reagent that is easier to handle. 10 Examples include melamine·6HF, pyridine·9HF, Et₃N·5HF, and the HF complexes of polyvinylpyridines. These complexed HF reagents allow for the direct hydrofluorination of alkenes, but they often display limited substrate generality with respect to different types of alkenes and/or poor functional group tolerance. Owing to the limited acidity of these reagents, some of the reactions can often take days to complete. In addition, several of these reagents remain commercially unavailable; thus, the handling of HF is necessary for their preparation prior to use.

Scheme 1. Background and Introduction

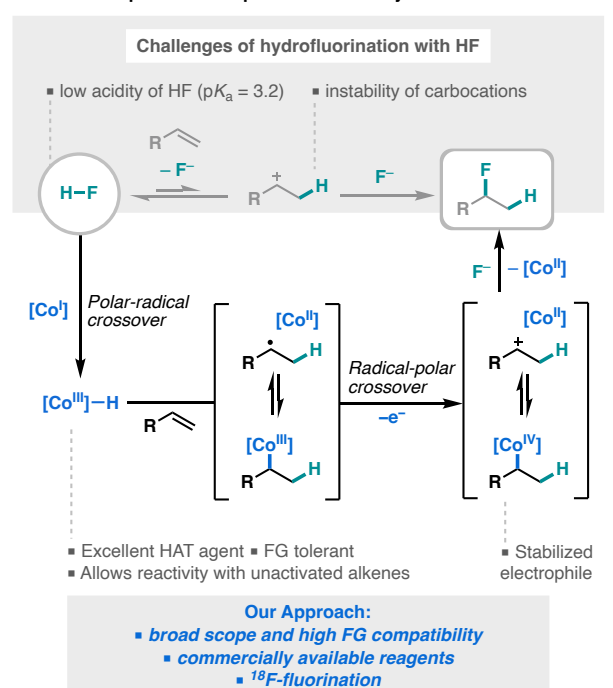
A. Prior art: radical hydrofluorination using hydride and electrophilic fluorine

$$R \stackrel{[M], [H^-]}{\sim} R \stackrel{[F^+]}{\sim} R \stackrel{[F^+]}{\sim} R$$

M = Co, Fe, Pd, Ni; [H⁻] = R₃SiH, NaBH₄; [F⁺] = selectfluor, NFSI requiring [H⁻] and [F⁺]; not amenable to radiofluorination

B. Prior art: polar hydrofluorination using HF complexes

C. This work: polar-radical-polar crossover hydrofluorination



Alternatively, alkene substrates could be directly activated to make carbocation intermediates, which can readily react with fluoride (Scheme 1B). Activation methods include the use of strong acids, 11 highly oxidizing photocatalyst, 12 and the combination of electrochemistry and palladium catalysis. 13 Most recently, Johnston and coworkers reported a Co(salen)-catalyzed alkene hydrofluorination reaction involving a 1,2-aryl shift using a combination of a hydrosilane and BF4 $^{-}$ as reagents. 14 These methods, while significantly expanding the toolbox for hydrofluorination reactions, are sensitive to the substitution patterns of alkenes; thus, these transformations are limited to a certain type of alkenes (e.g., styrenes or 1,1-disubstituted alkenes).

In this work, we describe the development of a redoxneutral hydrofluorination method that employs readily available Et₃N·3HF as the reagent. This reaction is enabled by the use of a family of Co(salen) type catalysts, which adopts Co^I, Co^{II}, and Co^{IV} oxidation states in the same catalytic cycle to facilitate the activation of Et₃N·3HF and the alkene in a polar-radical-polar crossover pathway towards Markovnikov hydrofluorination. This method has also been demonstrated for ¹⁸F-fluorination.

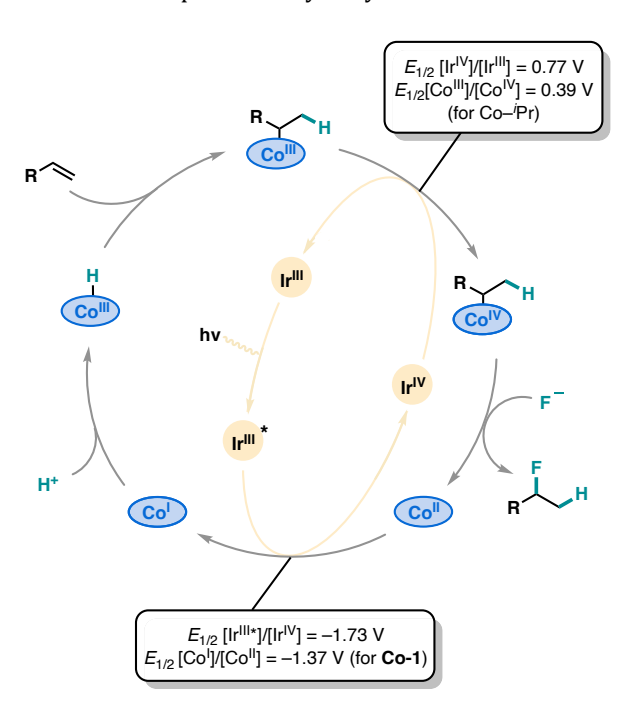
RESULTS AND DISCUSSION

Catalytic Strategy. To achieve alkene hydrofluorination using HF as the reagent, two main challenges need to be overcome. First, HF is poorly acidic and its reaction with a simple alkene is unfavorable (Scheme 1C, top). 15 Second, the prerequisite carbocation intermediate prior to nucleophilic fluorination is highly unstable and promiscuous, which will lead to poor chemoselectivity. To circumvent these issues, we propose a polar-radical-polar crossover approach leveraging metal-hydride-mediated HAT (MHAT; Scheme 1C, bottom). Specifically, the protonation of a Co^I intermediate will give rise to CoIII-H, which is a weakly acidic hydrogenatom source that will react readily with simple alkeneswhich are often nucleophilic-to generate a carbon-centered radical and a Co^{II} intermediate. These two species can undergo rapid and often reversible radical rebound to yield a Co^{III}-alkyl to complete the desired hydrometallation. Both the protonation and HAT steps are energetically feasible on thermodynamic and kinetic grounds, thereby making it possible the otherwise difficult activation of a simple alkene by HF. Advantageously, Co^{III}-H is known to readily react with a variety of alkenes with different substitution patterns,16 and its reactivity can be fine-tuned via ligand modification. These attributes may thus help overcome substrate scope limitations often encountered in previous hydrofluorination systems. Notably, the reductive generation of Co^{III}-H has been reported by our group¹⁷ and Baran group,¹⁸ in the context of alkene hydrofunctionalization, which has enabled deuteration, hydroarylation, and olefin isomerization reactions. In these systems, a weakly acidic proton source (e.g., HOAc, Et₃NH+BF₄-) was used to effect Co^{III}-H formation under chemical or electroreductive conditions in lieu of hydrosilanes or borohydrides.

The Co^{III}-alkyl intermediate generated from MHAT is often considered as an alkyl radical equivalent and not sufficiently electrophilic to react with a nucleophile. However, it

can subsequently be oxidized to Co^{IV}-alkyl, which constitutes a masked, stabilized carbocation that may undergo selective nucleophilic substitution. Indeed, the formation of Co^{IV}-alkyl complexes from corresponding Co^{III}-alkyl has recently been interrogated by Zhu,19 Ohmiya, 16 Kim,20 Zhang,²¹ Pronin,²² Holland, ²³ and Shigehisa²⁴ to enable nucleophilic substitution to form C-O, C-N, and C-C bonds. We envision that this reactivity may be extended to fluorination using F- as the nucleophile. In addition to the desired hydrofluorination product, this process will also generate a CoII species, which could be reduced to Co^I to close the catalytic cycle. Holistically, the Co-catalyzed hydrofluorination requires a single-electron oxidation step and a single-electron reduction step, and we proposed that a photocatalyst could be used to power this redox-neutral catalytic engine (Scheme 2).

Scheme 2. Proposed Catalytic Cycle



Discovery and Optimization. We chose 1,1-disubstitutedn alkene 1 as the model substrate and carried out an initial screening campaign, which led to the identification of optimal reaction conditions that provided an excellent 86% yield of the desired hydrofluorinated product **1-1** (Table 1). Co-1 was used as the MHAT catalyst, Ir(ppy)3 as the photocatalyst, 2,4,6-collidine as a catalytic proton shuttle, and commercially available Et₃N·3HF—a safer and practical surrogate of HF—as the fluoride and proton source. Indeed, Et₃N·3HF has been used to make fluorinated nucleoside glvcon on a 900-kg scale by Eli Lily in their manufacturing facility²⁵ and is used commonly in academic labs for preparative scale synthesis.26 In this system, Ir(ppy)3 has an excited state reduction potential of $E_{1/2}$ [IrII*]/[IrIV] = -1.73 V vs SCE) and its reductively quenched congener has an oxidation potential of $E_{1/2}$ [Ir^{IV}]/[Ir^{III}] = 0.77 V vs SCE.²⁷ Thus, $Ir(ppy)_3$ is capable of reducing $Co^{II}(salen)$ ($E_{1/2}[Co^{II}]/[Co^{II}] =$ -1.37 V vs SCE for **Co-1**; see Figure S8 for cyclic voltammetry data), and its oxidized form is sufficiently potent to convert Co^{III} -alkyl to Co^{IV} -alkyl ($E_{1/2}[Co^{III}]/[Co^{IV}] = 0.39 \text{ V vs}$

SCE when alkyl = 4 Pr in DCM). 23 This method effectively adds HF across a simple alkene via a polar-radical-polar pathway, which is appealing from an atom-economy perspective vs prior methods using hydride and/or electrophilic fluorine agents.

Table 1. Optimization of Reaction Conditions^a

Entry	Variation	Yield (%)
1	None	86
2	No Co-1	0
3	No photocatalyst	0
4	No light	0
5	No 2,4,6-Collidine	3
6	4CzIPN (2) instead of Ir(ppy) ₃	8
7	Phenoxazine (3) instead of Ir(ppy) ₃	15
8	DCE instead of DCM	73
9	4 equiv of KF instead of Et ₃ N•3HF	5
10	4 equiv Olah's reagent instead of Et ₃ N•3HF	0
11	1 equiv of Et ₃ N•3HF	50
12	2,6-Lutidine instead of 2,4,6-collidine	80
13	440 nm Kessil lamp instead of Lumidox	54
14	12 hours instead of 24 hours reaction	79

$$^{t}Bu$$
 ^{t}Bu
 $^$

^a0.2 mmol scale. ^bYields determined by ¹⁹F NMR using 1-fluoronapthalene as the internal standard.

Control experiments without light, photocatalyst, or cobalt salen catalyst gave no product (Table 1, entries 2–4). Without collidine, only traces of **1-1** was observed (entry 5); we hypothesize that collidinium ion formed in situ is responsible for the protonation of Co¹, which is more efficient compared to Et₃N·3HF, likely due to the higher acidity of collidinium in DCM.²⁸ Using organic reductive photocatalysts 4CzlPN **2** $(E_{1/2} [2^*]/[2^+] = -1.18$ V vs SCE)^{26b} or phenoxazine derivative **3** $(E_{1/2} [3^*]/[3^+] = -1.93$ V vs SCE),²⁹ substantially diminished yields were obtained³⁰ (entries 6-7). Changing the solvent from DCM to DCE led to a small decrease in yield (entry 8). Upon testing other fluoride sources, we found that KF provided 5% yield of desired **1-1**

where Olah's reagent (i.e., pyridine hydrofluoride) gave no product formation (entries 9-10). The loading of Et₃N·3HF could be decreased to 1 equiv with satisfactory yield (entry 11). Substituting 2,4,6-collidine with 2,6-lutidine did not affect the reaction efficiency (entry 12). We also found that the reaction conversion was nearly complete in 12 hours (entry 13). Finally, switching the light source from Lumidox to a Kessil lamp led to a diminished 54% yield (entry 14).

To assess the substrate generality of our hydrofluorination strategy, a panel of alkene substrates featuring different degrees of substitution were tested under the optimal conditions described above, including α -olefin 4, isoprenyl 5, styrenyl 6, and 1,2-disubstituted alkene 7. However, the desired products were observed in substantially reduced quantities (Scheme 3A, top). These findings are not surprising, given that these alkenes feature distinct steric and electronic characteristics and thus may require tailored Co(salen) catalysts to achieve optimal efficiency in the MHAT and nucleophilic substitution processes. Indeed, we have previously observed differences in the relative rates of MHAT depending on the catalyst and the alkene structure by means of differential electrochemical mass spectrometry (DEMS) measurements. 17

Leveraging the structural modularity of salen ligands, we then interrogated the structure-activity relationships between the catalyst and each class of alkenes using the high-throughput experimentation (HTE) technology. Micromolar scale (0.0175 mmol) 24-well plates were designed and carried out to assess multiple cobalt catalysts with the aforementioned four classes of alkenes, and the data of catalysts screening of mono-substituted alkene 4 are presented as a heat map in Scheme 3B (For structure of each cobalt salen catalysts, please see Figure S3).

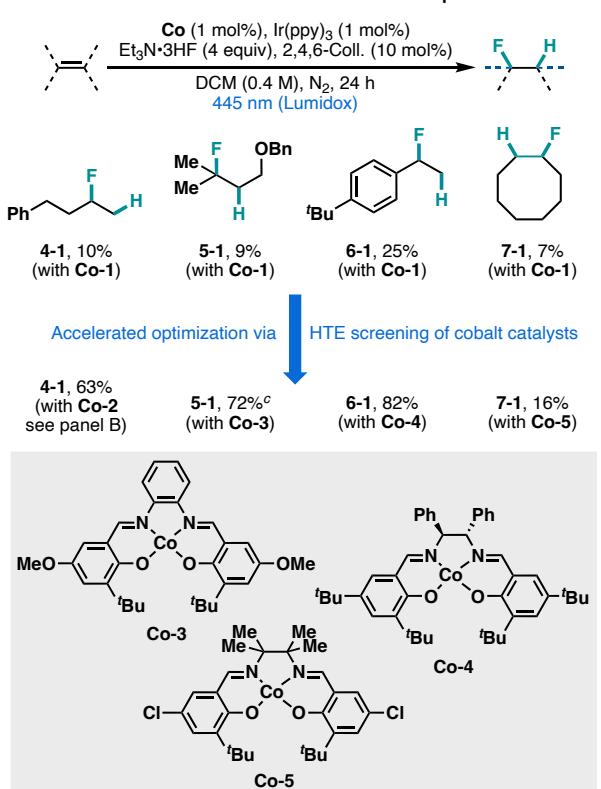
Co-2 with electron-withdrawing CF₃ groups on the salicylaldehyde portions of the ligand was identified as optimal for unactivated monosubstitued alkenes, giving the product 4-1 in 67% yield. In general, the HTE data show that more electron-deficient Co(salen) catalysts Co-2, Co-11, and Co-18 provided higher reactivity for 4 (Scheme 3B). We hypothesize that the Co^{III}–H intermediates from such catalysts display enhanced acidity and electrophilicity, and it is thus capable of engaging less electron-rich α -olefins in MHAT. In addition, it is possible that improved electrophilicity of the Co^{IV}–alkyl generated upon hydrometallation and oxidation permits more efficient nucleophilic substitution with F-Scaling up this reaction by \sim 10 fold (0.2-mmol) gave 63% yield with 5 mol% catalyst loading (Table 3), showing good consistency with HTE results.

In other optimization sets, more electron-rich and sterically less encumbered **Co-3** (vs. **Co-1**) appeared to efficiently mediate the reaction with isoprenyl alkene **5**—an electronically activated yet sterically hindered substrate—with an improved yield of 72% (Scheme 3A, bottom). In addition, **Co-4** was identified as a lead catalyst for styrenyl alkenes **6**, affording 82% yield of the desired benzyl fluoride **6-1**. Nevertheless, 1,2-disubstituted alkenes **7** remained recalcitrant to extensive catalyst optimization, only showing a marginally improved yield of 16% using **Co-5** catalyst.

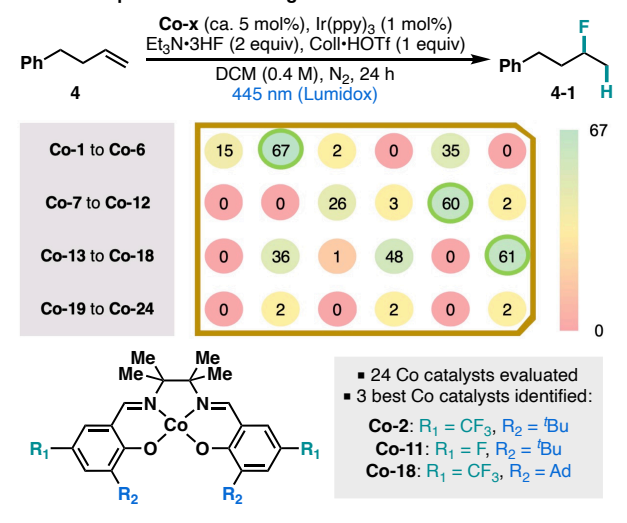
Further fine-tuning of reaction conditions for each class of alkenes using their respective optimal catalyst was also performed to further boost the yield (see Table S4-8). These results demonstrated the advantage of employing structurally modular Co(salen) complexes in the desired hydrofluorination reaction and exemplified the power of HTE in enabling rapid reaction optimization.

Scheme 3. Establishing substrate generality with respect to alkene substitution. (A) Reaction of alkenes with different substitution patterns under initially optimal conditions and further optimized conditions. (B) An example of high throughput experimentation for Co(salen) catalyst screening for substrates with different degrees of substitution.

A. Reactions of alkenes with different substitution patterns^{a,b}



B. An example of HTE screening for alkene $5^{b,d}$



^a0.2 mmol scale. ^bYields determined by ¹⁹F NMR using 1-fluoronapthalene as the internal standard, unless otherwise noted. ^cIsolated yields. ^d0.0175mmol scale.

Scope Elucidation. With the optimal reaction conditions in hand, we next explored the substrate scope of our methodology (Tables 2-5). We note that due to very similar polarity of some of the fluorination products compared with their respective starting alkenes, yields determined via quantitative NMR were reported in these cases to more accurately reflect the reaction efficiency, with the identity of the products further confirmed by means of isolation and/or 2D NMR analysis.

Panels of alkenes with varying degrees of substitution and skeletal and functional diversity were transformed to corresponding fluoroalkanes smoothly. Substrates bearing sulfonamide (9), imide (12), and amide (13) groups were converted efficiently without the reduction of these potentially sensitive functional groups. For the imide substrate, only 5% yield could be observed using the original optimal catalyst Co-1; however, switching to Co-3 catalyst boosted the yield to 40%. Furthermore, running the reaction in an NMR tube increased the yield to 60%, likely as a result of enhanced light penetration. Interestingly, for limonene (14) bearing two different types of alkenes, the catalyst was highly selective for the hydrofluorination of the terminal alkene, giving product 14-1 in 34% yield with only 2% of speculative hydrofluorination of the internal alkene.

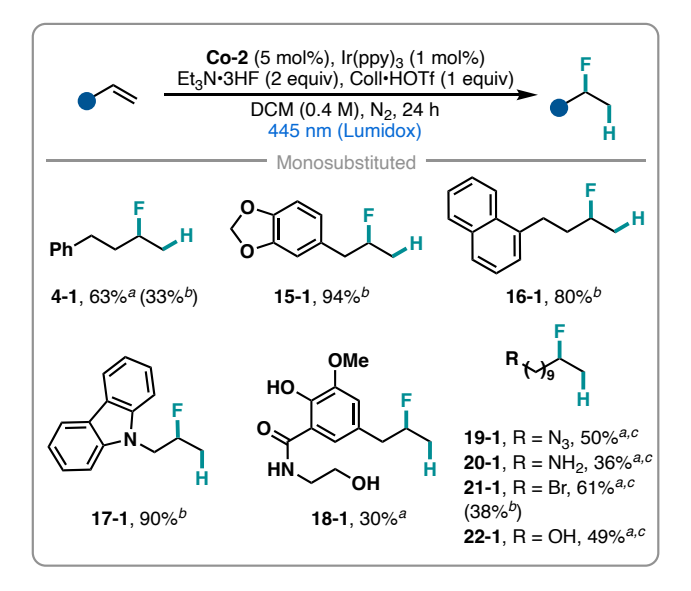
Table 2. Scope of 1,1-Disubstituted Alkenes.

^aYields determined by ¹⁹F NMR using 1-fluoronapthalene as the internal standard. ^bIsolated yield. ^cReaction ran in an NMR tube, see supporting information for details. ^dUse 1 mol% of **Co-3** instead of **Co-1**.

For mono-substituted alkenes (Table 3), substrates bearing carbozole (17), free alcohol (18, 22), azide (19), free amine (20) and reductively labile alkyl bromide (21) groups could be converted to the desired hydrofluorinated product in moderate to excellent yields. Natural products

such as safrole (15) and biologically active compound alibendol (18) can also undergo transformation efficiently to deliver the fluoroalkane products.

Table 3. Scope of Mono-substituted Alkenes.



^aYields determined by ¹⁹F NMR using 1-fluoronapthalene as the internal standard. ^bIsolated yield. ^cReaction ran in an NMR tube, see supporting information for details.

For isoprenyl alkenes, excellent functional group tolerance was also observed. Substrates featuring ether (5, 23, 25, 28), ester (24), Boc-protected amine (23, 30), free alcohol (29), carbamate (26, 27), and pyrimidine (25) groups were converted smoothly to the desired products. For product 29-1, we observed excellent regioselectivity favoring hydrofluorination of the acyclic alkene with no detectable functionalization of the endocyclic alkene. The reaction efficiency for a number of isoprenyl substrates were low when running the reaction in glass vials (see Table S9), but that switching the reaction vessel to NMR tubes led to significantly improved yield likely as a result of increased light penetration. For example, substrate 23 was converted to 23-1 in 57% yield with a glass vial, which was improved to 86% when using an NMR tube instead.

Table 4. Scope of Isoprenyl Alkenes.

^aYields determined by ¹⁹F NMR using 1-fluoronapthalene as the internal standard. ^bIsolated yield. ^cReaction ran in an NMR tube, see supporting information for details. ^dIsolated as a mixture of 2 diastereomers because the substrate used was a mixture of diastereomers. ^eNo cycloetherification product was observed by NMR analysis.

Lastly, we also demonstrated that vinylarenes were excellent substrates in this reaction (Table 5). Pyridine (31), Bpin (33), and amide (34) groups were compatible, and internal alkene (32) also furnished the desired product in good yield. Due to the known lability of benzylic fluorides, several reaction yields here were determined using ¹⁹F NMR with the product structures further confirmed by means of 2D NMR analysis. At this stage, 1,2-disubstituted alkenes and tetrasubstitued alkenes remain challenging substrates in our reaction system (Figure S4).

The observation that different alkenes perform optimally with a different Co catalyst pointed to the possibility that tunable chemoselectivity may be achieved for systems bearing two distinct types of alkenes. We obtained preliminary proof of principle in intermolecular competition experiments, demonstrating that the selectivity could be overturned via catalyst selection (see SI section 6). We will continue to leverage the high structurally tunability of Co(salen) catalysts to investigate chemo- and regioselective hydrofluorination in complex systems.

Table 5. Scope of Styrenes.

 a Yields determined by 19 F NMR using 1-fluoronapthalene as the internal standard. b Isolated yield.

¹⁸F-Hydrofluorination. The synthetic importance of this methodology was further demonstrated in a series of ¹⁸Fhydrofluorination reactions that are potentially applicable in positron emission tomography (PET) imaging. PET is a non-invasive imaging technique used to probe biological processes in vivo via the administration of a positron-emitting radiotracer. PET imaging has been used for the purpose of diagnosing and monitoring the progression of diseases, as well as aiding in the development of drugs, both in the preclinical and clinical stages.3 Thus, the development of new synthetic strategies to prepare new PET tracers is highly desirable. Radiofluorination strategies often utilize readily available [18F]fluoride as the most common 18F source with high molar activity. Due to the relatively short half-life of ¹⁸F (half-life = 109.8 min), ^{3e 18}F-fluorination reactions ideally should take no more than 30 minutes.

In this context, we showed that our methodology can be successfully applied to ¹⁸F-labeling of alkenes substrates. The reaction was further optimized to be compatible with [18F]fluoride that can be conveniently generated from a medical cyclotron. Specifically, an aqueous solution of [18F]fluoride was passed through an ion exchange resin loaded with Et₄NHCO₃ to furnish [18F]Et₄NF that is azeotropically dried and re-solubilized in an organic solvent. The protocol was carried out typically using 18.5-37 MBq (0.5-1mCi) of [18F]Et₄NF, and the radiochemical conversion (RCC) was analyzed after 20 minutes of reaction. We found that under modified conditions, alkene 1 was converted to the ¹⁸F-hydrofluorinated product [¹⁸F]**1-1**with a satisfying RCC of 24% (Table 6, entry 1). Using less polar DCM or more polar DMF and DMSO as the solvent leads to diminished RCCs (entries 2-4). Changing the base for the ion exchange resin or running the reaction for shorter and longer times both gave lower RCCs (entries 5-8).

Table 6. Development of ¹⁸F-Hydrofluorination Protocol

Entry	Variation	RCC (%) ^{a,b}
1	None	24
2	DCM instead of MeCN	8
3	DMF instead of MeCN	1
4	DMSO instead of MeCN	1
5	K ₂ CO ₃ /K ₂₂₂ instead of Et ₄ NHCO ₃	3
6	Me ₄ NHCO3 instead of Et ₄ NHCO ₃	4
7	10 min instead of 20 min	12
8	30 min instead of 20 min	14

^a0.01 mmol scale. ^bRCC was determined by radio-TLC.

We subsequently expanded the scope of the ¹⁸F-hydrofluorination reaction to a variety of alkene substrates including those derived from biologically active compounds (Table 7). For example, alibendol (**18**), an antispasmodic, choleretic, and cholekinetic,³¹ was ¹⁸F-hydrofluorinated with favorable RCC. In addition, vinylpyridine (**31**) and amide-bearing styrene (**34**) were transformed into desired products with moderate to good RCCs. Given the natural abundance and synthetic availability of alkenes, this methodology will provide a new avenue for the synthesis of ¹⁸Flabeled tracers for PET imaging applications.

Table 7. Scope of ¹⁸F-Hydrofluorination Reaction^a

^a0.01 mmol scale. ^b5 mol% **Co-2** was used instead of **Co-1**. ^c5 mol% **Co-4** was used instead of **Co-1**.

Mechanistic Investigations. A series of photochemical, electroanalytical, and physical organic chemistry studies were performed to probe the proposed reaction mechanism. Stern-Volmer studies showed that the fluorescence of Ir^{III*} is quenched by **Co-1** catalyst (Figure S20), whereas its quenching by collidinium triflate or substrate **1**, **4**, and **6** takes place at a rate too low to produce observable luminescence quenching (Figures S21-24). Considering that the reduction potential of substrates **1** and **4** is below –3.4 V vs. Fc/Fc+ (Figures S9-10) and that of **6** was measured to be – 3.2 V vs. Fc/Fc+ (Figure S11), which is about 1 V more negative than $E_{1/2}$ [Ir^{III*}]/[Ir^{IV}], we propose that it is most likely that Co^{II} is reduced to Co^I by the excited iridium photocatalyst and that direct activation of alkene does not contribute to the observed reactivity.

Upon the formation of intermediate I, There are two possible pathways (Scheme 4A): I could undergo cage escape and then be oxidized by IrIV to generate carbocation III $(E_{1/2}^{\text{ox}} = 0.09 \text{ V for } tert\text{-butyl radical});^{32}$ alternatively, the cage-collapsed Co^{III}-alkyl species II could be readily oxidized to form Co^{IV} -alkyl species **IV** ($E_{1/2}$ [Co^{III}]/[Co^{IV}] = 0.39 V when alkyl = ${}^{i}Pr^{24}$). Both intermediates **III** and **IV** can undergo fluorination via pathway **a** and pathway **b**, respectively). As direct evidence supporting the presence of a nucleophilic substitution step in the catalytic cycle, substrates 35 and 36 underwent unexpected rearrangement via neighboring group participation, yielding products 35-2 and 36-2 in addition to direct hydrofluorination products 35-1 and **36-1** (Scheme 5). In these reactions, competitive substitution with the pendant carbonyl group in the substrate likely takes place prior to fluoride attack. In contrast, when a substrate with a longer alkyl linker between the alkene and the carbonyl group (37) was subject to the reaction, no rearrangement product was detected. These results support a radical-polar crossover mechanism for the fluorination process. However, it cannot distinguish between pathways a

Through further voltammetry studies and DFT calculations, we found that both pathways $\bf a$ and $\bf b$ are likely operating in the reaction, and that the contribution of each pathway to the observed overall reactivity depends on the type of alkene substrate used.

Previous reports suggest that an equilibrium exists between Co^{III}-alkyl (II) and the neutral alkyl radical (I) (equilibrium constant K_{eq1} ; Scheme 4A).^{17, 33, 34} The direction of the equilibrium and magnitude of K_{eq1} varies with different Co(salen) catalysts and alkene substrates. To make a qualitative assessment of the fluorination mechanism, rotating disk electrode (RDE) voltammetry experiments were performed using Co-2 catalyst. This complex showed a reversible redox wave at -1.7 V vs Fc/Fc+,35 which was assigned to the Co^{II}/Co^I couple. The addition of collidinium triflate (Coll-HOTf) as the proton source led to an irreversible reduction wave and substantial current enhancement at this potential, the magnitude of which increased as the concentration of the protic acid increased from 5 mM to 100 mM (Scheme 4B). This observation is consistent with the generation of Co^{III}–H intermediate via reduction of Co^{II} to Co^I followed by protonation. As Co^{III}-H of this type is known to mediate hydrogen evolution reaction (HER) in the absence of an alkene substrate, 36 a catalytic current is seen. When using Et₃N·3HF as the proton source instead of Coll·HOTf, no catalytic current was observed (Figures S17-18), further supporting our hypothesis that collidinium ion generated in situ is responsible for the protonation of Col species.

Notably, when mono-substituted alkene 4 was added to the mixture of Co-2 and 100 mM collidinium triflate, a decrease in the intensity of the catalytic current was observed (Scheme 4D). This result indicates that the aforementioned HER is inhibited in the presence of 4, as the equilibrium post-HAT (K_{eq1}) favors Co^{III}-alkyl, a species that cannot be further reduced at a potential of -1.7 V vs. Fc/Fc+.37,38 To further validate this hypothesis, we computed the association free energy of Co^{II}/isopropyl radical pair to Co^{III}-ⁱPr to be kcal/mol at the SMD(DCM)/M06-L/def2-TZVPP/W06//SMD(DCM)/M06-L/def2-SVP/W06 level³⁹ (Scheme 4D), suggesting that the equilibrium indeed favors the secondary Co^{III}-alkyl species for mono-substituted alkenes (e.g., 4).

In stark contrast, when 1,1-disubstituted alkene **1** was added to the same solution of **Co-2** and collidinium triflate, further current enhancement was observed (Scheme 4C). This result indicates that Co^{II} is regenerated at a greater rate in the presence of the alkene, which could be a result of two contributing factors: (i) Co^{III}–H participates in MHAT to an alkene at a faster rate than HER,⁴⁰ and (ii) the equilibrium $K_{\rm eq1}$ favors formation of the Co^{III}/alkyl radical pair over the Co^{III}–alkyl adduct. Furthermore, our DFT calculations suggest that the association free energy of Co^{III}/tert-butyl radical pair to form Co^{III}– t Bu is 2.9 kcal/mol (Scheme 4C), indicating that the equilibrium favors the Co^{III}/alkyl radical pair for 1,1-disubstituted alkenes (e.g., **1**).

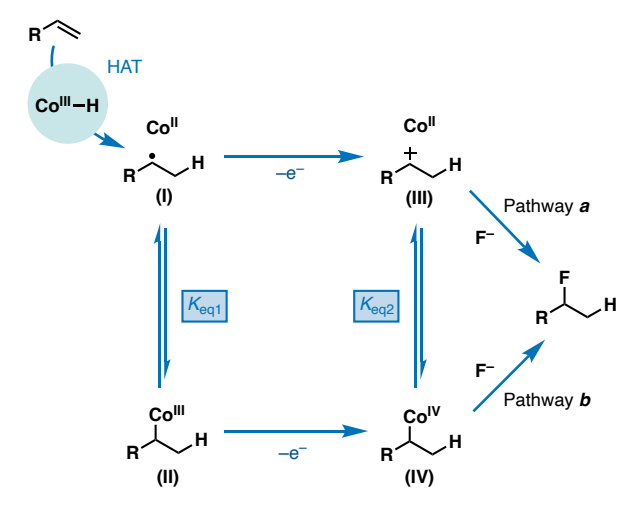
We attribute the different behaviors of $\bf 1$ and $\bf 4$ in RDE experiments to the shift of equilibrium $K_{\rm eq1}$, which is influenced by the relative stability of alkyl radicals with varying degrees of substitution (i.e., a tertiary alkyl radical is generally more stable than a secondary alkyl radical).

DFT calculations further demonstrated that after the oxidation event, another equilibrium exists between the resultant Co^{IV}-alkyl (IV) and a Co^{II}/carbocation pair (III) (equilibrium constant K_{eq2} ; Scheme 4A). For tertiary Co^{IV}-alkyl species, the dissociation is nearly barrierless (the computed barrier ΔE^{\ddagger} is 0.2 kcal/mol for Co^{IV} $_{-t}$ Bu) and exergonic (the computed free energy change ΔG is -12.4 kcal/mol for Co^{IV}-^tBu), strongly favoring the formation of Co^{II} and carbocation (Scheme 6A).41 Thus, if tertiary Co^{IV}-alkyl is generated via the oxidation of Co^{III}-alkyl by Ir^{IV}, it would undergo dissociation readily. The subsequent reaction between a carbocation (formed via either direct oxidation of alkyl radical (I) or dissociation of Co^{IV}-alkyl) and F- should be facile (estimated to be a diffusion-controlled process⁴²) and irreversible. Therefore, we conclude that 1,1-disubstituted and trisubstituted alkenes undergo hydrofluorination via pathway a. In contrast, pathway b in this scenario would require either a sluggish S_N2 reaction at a tertiary carbon center or a difficult reductive elimination from a Co center without naturally available cis-coordination sites.

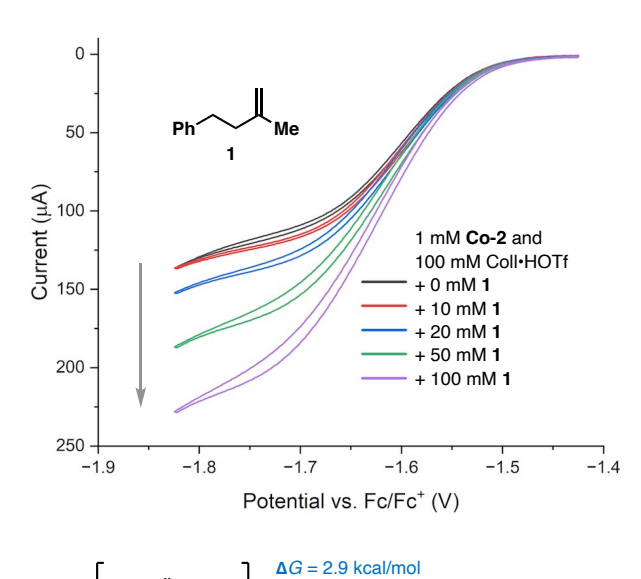
On the other hand, for mono-substituted alkenes, the equilibrium K_{eq2} favors the formation of secondary Co^{IV} -alkyl species with a computed dissociation free energy of 10.6 kcal/mol (Scheme 6B). In comparison with the highly endergonic dissociation, fluorination of Co^{IV}-alkvl via an S_N2 mechanism has a low activation free energy of 1.9 kcal/mol. As a result, pathway **b** is favored over pathway **a** and likely the predominant mechanism for reactions with mono-substituted alkenes.⁴³ This hypothesis is supported by literature reports showing that enantioselective nucleophilic substitution of secondary Co^{IV}-alkyl can be achieved with alcohols and amines using chiral Co(salen) complexes, 20a, 21, ^{22b, 24} which would not be plausible if these transformations proceed through a carbocation pathway. Future work will focus on further elucidation of divergent mechanistic pathways with an ultimate goal of facilitating the discovery of novel hydrofunctionalization reactions using a similar strategy.

Scheme 4. Mechanistic investigation using voltammetry.

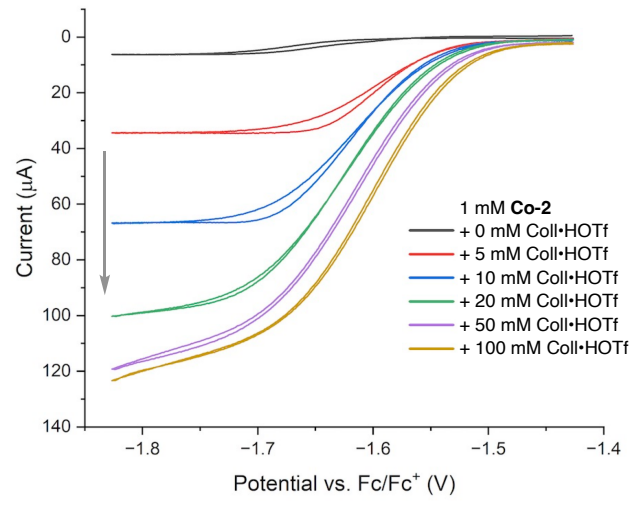
A. Proposed pathways for nucleophilic fluorination



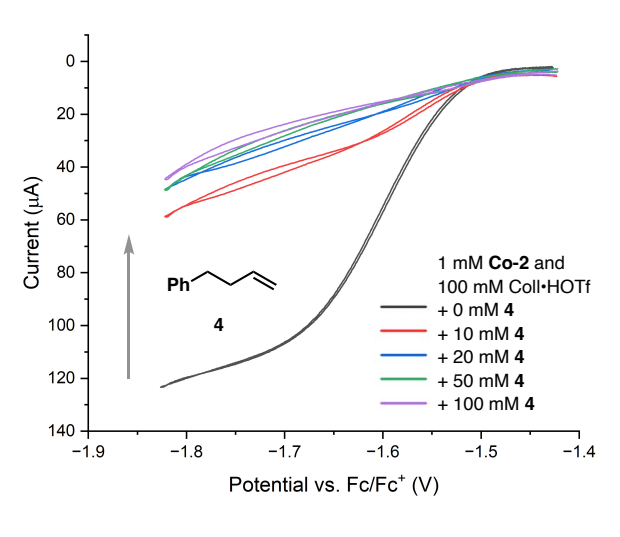
C. RDE voltammetry data of Co^{III}–H with varying amounts of 1



B. RDE voltammetry data of Co-2 with varying amounts of acid



D. RDE voltammetry data of Co^{III}-H with varying amounts of 4



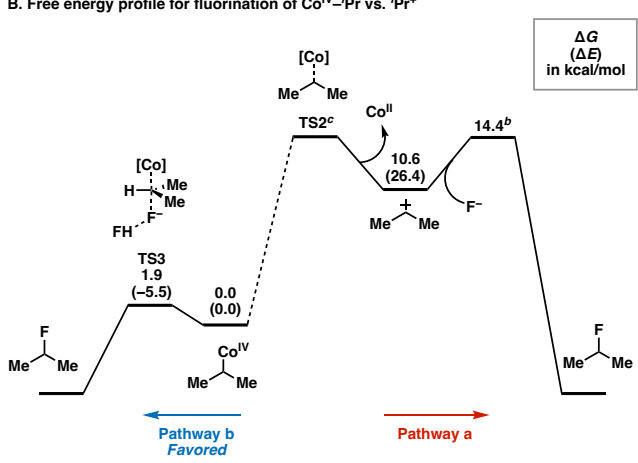
Scheme 5. Carbocation rearrangement experiments.

^aYields determined by ¹⁹F NMR using 1-fluoronapthalene as the internal standard. bIsolated yields.

Scheme 6. DFT-computed free energy profiles for the fluorination step.a

A. Free energy profile for fluorination of CoIV_tBu vs. tBu+

B. Free energy profile for fluorination of Co^{IV}_ⁱPr vs. ⁱPr+



^aCo-2 was used in the calculations in panel A. In panel B, a truncated model of Co-2 without substituents on the diamine backbone or salicylaldehyde units was used, as the transition state search for the S_N2 step of the full catalyst did not converge. See SI section 10 for details. bThe effective activation free energy for a diffusion-limited ion combination was estimated to be 3.8 kcal/mol.⁴² ^cWe were unable to locate the dissociation transition state since the potential energy increases monotonically along with the cleavage of the Co-C bond.

CONCLUSION

In conclusion, we have developed Co(salen)-catalyzed hydrofluorination of alkenes via a polar-radical-polar crossover mechanism. Commercially available and inexpensive Et₃N·3HF is used as both the proton and fluoride donor, thus avoiding the use of silanes and electrophilic fluorine sources. This methodology shows a broad substrate generality and tolerates unactivated alkenes and styrenes with varying degrees of substitution and diverse functional groups. This methodology is also successfully applied to the ¹⁸F-labeling of several biologically active compounds using readily available [18F]fluoride with satisfying radiochemical conversion. Mechanistic investigations confirm the intermediacy of radical and carbocation intermediates and their respective Co complexes in the proposed catalytic cycle. Further, divergent pathways are identified for the nucleophilic fluorination step, wherein the contribution of each pathway depends on the structure of the alkene substrates. Future efforts will be directed towards gaining a deeper understanding of the reaction mechanism and extending the same catalytic strategy to other synthetically valuable hydrofunctionalization reactions.

ASSOCIATED CONTENT

Supporting Information. This material is available free of charge via the Internet at http://pubs.acs.org. Experimental procedures, analytical data, and NMR spectra (PDF)

AUTHOR INFORMATION

Corresponding Author

Steven H. Liang – Department of Radiology and Imaging Sciences, Emory University, Atlanta, Georgia 30322, United States; orcid.org/0000-0003-1413-6315; Email: steven.liang@emory.edu

Song Lin – Department of Chemistry and Chemical Biology, Cornell University, Ithaca, New York 14853, United States; orcid.org/0000-0002-8880-6476; Email: songlin@cornell.edu

Authors

Jinjian Liu – Department of Chemistry and Chemical Biology, Cornell University, Ithaca, New York 14853, United States; orcid.org/0000-0003-4367-7874

Jian Rong – Department of Radiology and Imaging Sciences, Emory University, Atlanta, Georgia 30322, United States; orcid.org/0000-0002-3960-1669

Devin P. Wood – Department of Chemistry and Chemical Biology, Cornell University, Ithaca, New York 14853, United States

Notes

The authors declare no competing financial interest.

ACKNOWLEDGMENT

This work was supported by the National Science Foundation through the NSF-DFG Lead Agency Activity in Electrosynthesis and Electrocatalysis (CHE-2055451 to S.L.). This study made use of the Cornell University NMR facility supported by the National Science Foundation (CHE-1531632). S.H.L. gratefully acknowledges the support provided, in part, by the NIH grants (NS130128, AG081401), Emory Radiology Chair Fund and Emory School of Medicine Endowed Directorship. We thank Dr. Yi Wang for DFT calculations and discussion. We thank Dr. Ivan Keresztes and Dr. Wen Zhang for NMR data analysis. We thank Dr. Xiangyu Wu for discussion and assistance with catalyst synthesis. We thank Dr. Dylan Boucher for discussion on RDE experiments. We thank Blake Weeks for assistance with substrate synthesis. We thank Jonas Rein for data reproduction. We thank Dr. Luiz F. T. Novaes for reviewing data and editing graphics.

REFERENCES

- (1) For selected reviews on applications of organofluorine compounds, see: (a) Ismail, F. M. D. Important Fluorinated Drugs in Experimental and Clinical Use. J. Fluor. Chem. 2002, 118, 27-33. (b) Isanbor, C.; O'Hagan, D. Fluorine in Medicinal Chemistry: A Review of Anti-Cancer Agents. J. Fluorine Chem. 2006, 127, 303-319. (c) Bégué, J.-P.; Bonnet-Delpon, D. Recent Advances (1995-2005) in Fluorinated Pharmaceuticals Based on Natural Products. J. Fluorine Chem. 2006, 127, 992-1012. (d) Hagmann, W. K. The Many Roles for Fluorine in Medicinal Chemistry. J. Med. Chem. 2008, 51,4359-4369. (e) Purser, S.; Moore, P. R.; Swallow, S.; Gouverneur, V. Fluorine in Medicinal Chemistry. Chem. Soc. Rev. 2008, 37, 320-330. (f) Wang, J.; Sánchez-Roselló, M.; Aceña, J. L.; del Pozo, C.; Sorochinsky, A. E.; Fustero, S.: Soloshonok, V. A.: Liu, H. Fluorine in Pharmaceutical Industry: Fluorine-Containing Drugs Introduced to the Market in the Last Decade (2001-2011). Chem. Rev. 2014, 114, 2432-2506. (g) Champagne, P. A.; Desroches, J.; Hamel, J.-D.; Vandamme, M.; Paquin, J.-F. Monofluorination of Organic Compounds: 10 Years of Innovation. Chem. Rev. 2015, 115, 9073-9174. (h) Zhang, C.; Yan, K.; Fu, C.; Peng, H.; Hawker, C. J.; Whittaker, A. K. Biological utility of fluorinated compounds: from materials design to molecular imaging, therapeutics and environmental remediation. Chem. Rev. 2022, 122, 167-208. (i) Patel, C.; André-Joyaux, E.; Leitch, J. A.; de Irujo-Labalde, X. M.; Ibba, F.; Struijs, J.; Ellwanger, M. A.; Paton, R.; Browne, D. L.; Pupo, G.; Aldridge, S.; Hayward, M. A.; Gouverneur, V. Fluorochemicals from fluorspar via a phosphate-enabled mechanochemical process that bypasses HF. Science 2023, 381, 302-306.
- (2) Inoue, M.; Sumii, Y.; Shibata, N. Contribution of Organo-fluorine Compounds to Pharmaceuticals. *ACS Omega* **2020**, 5, 10633–10640.
- (3) For selected reviews on PET imaging techniques, see: (a) Phelps, M. E. Positron emission tomography provides molecular imaging of biological processes. Proc. Natl. Acad. Sci. U. S. A. 2000, 97, 9226- 9233. (b) Ametamey, S. M.; Honer, M.; Schubiger, P. A. Molecular imaging with PET. Chem. Rev. 2008, 108, 1501-1516. (c) Willmann, J. K.; van Bruggen, N.; Dinkelborg, L. M.; Gambhir, S. S. Molecular Imaging in Drug Development. Nat. Rev. Drug Discovery 2008, 7, 591-607. (d) Preshlock, S.: Tredwell, M.: Gouverneur, V. ¹⁸F-labeling of arenes and heteroarenes for applications in positron emission tomography. Chem. Rev. 2016, 116, 719-766. (e) Deng, X.; Rong, J.; Wang, L.; Vasdev, N.; Zhang, L.; Josephson, L.; Liang, S. H. Chemistry for Positron Emission Tomography: Recent Advances in ¹¹C-, ¹⁸F-, ¹³N-, and ¹⁵O- Labeling Reactions. Angew. Chem., Int. Ed. 2019, 58, 2580-2605. (f) Rong, I.; Haider, A.; Jeppesen, T.E.; Lee, J.; Steven H. Liang, S.H. Radiochemistry for positron emission tomography. *Nat Commun* **2023**, 14, 3257. (4) (a) Barker, T. I.; Boger, D. L. Fe(III)/NaBH₄-Mediated Free Radical Hydrofluorination of Unactivated Alkenes. I. Am. Chem. Soc. 2012, 134, 13588-13591. (b) Shigehisa, H.; Nishi, E.; Fuiisawa, M.: Hirova, K. Cobalt-Catalyzed Hydrofluorination of Unactivated Olefins: A Radical Approach of Fluorine Transfer. Org. Lett. 2013, 15, 5158-5161. (c) Emer, E.; Pfeifer, L.; Brown, J. M.; Gouverneur, V. cis-Specific Hydrofluorination of Alkenylarenes under Palladium Catalysis through an Ionic Pathway. Angew. Chem., Int. Ed. 2014, 53, 4181-4185. (d) Xie, Y.; Sun, P. W.; Li, Y.; Wang, S.; Ye, M.; Li, Z. Ligand-Promoted Iron(III)-Catalyzed Hydrofluorination of Alkenes. *Angew*. Chem., Int. Ed. 2019, 58, 7097-7101. (e) Song, P.; Zhu, S.; Nickel-Catalyzed Hydrofluorination of Unactivated Alkenes through a HAT Pathway. ACS Catalysis 2020, 10, 13165-13170. (f) Yin, X.-M.; Chen, B.; Qiu, F.; Wang, X.-H.; Liao, Y.; Wang, M.;

- Lei, X.-X.; Liao, J. Enantioselective Palladium-Catalyzed Hydro-fluorination of Alkenylarenes. *ACS Catal.* **2020**, 10, 1954–1960. (5) Shevick, S. L.; Wilson, C. V.; Kotesova, S.; Kim, D.; Holland, P. L.; Shenvi, R. A. Catalytic hydrogen atom transfer to alkenes: a roadmap for metal hydrides and radicals. *Chem. Sci.* **2020**, 11, 12401–12422.
- (6) Meyer, D.; Jangra, H.; Walther, F.; Zipse, H.; Renaud, P. A third generation of radical fluorinating agents based on N-fluoro-N-arylsulfonamides. *Nat. Commun.* **2018**, 9, 4888.
- (7) Jacobson, O.; Kiesewetter, D. O.; Chen, X. Fluorine-18 Radiochemistry. Labeling Stategies and Synthetic Routes *Bioconjugate Chem.* **2015**, 26, 1–18.
- (8) (a) Pupo, G.; Gouverneur, V. Hydrogen Bonding Phase-Transfer Catalysis with Alkali Metal Fluorides and Beyond. *J. Am. Chem. Soc.* **2022**, 144, 12, 5200–5213. (b) Pupo, G.; Ibba, F.; Ascough, D. M. H. H.; Vicini, A. C.; Ricci, P.; Christensen, K. E.; Pfeifer, L.; Morphy, J. R.; Brown, J. M.; Paton, R. S.; Gouverneur, V. Asymmetric Nucleophilic Fluorination under Hydrogen Bonding Phase-Transfer Catalysis. *Science* **2018**, 360, 638.
- (9) Bertrand, X.; Chabaud, L.; Paquin, J.-F. Hydrofluorination of Alkenes: A Review. *Chem.*—*Asian J.* **2021**, 16, 563–574.
- (10) (a) Olah, G. A.; Nojima M.; Kerekes I. Hydrofluorination of Alkenes, Cyclopropane and Alkynes with Poly-Hydrogen Fluoride/Pyridine (Trialkylamine)Reagents. Synthesis 1973, 779-780. (b) N. Yoneda, T. Abe, T. Fukuhara, A. Suzuki, Melamine-hydrogen fluoride solution. A highly effective and convenient hydrofluorination reagent of alkenes. Chem. Lett. 1983, 12, 1135-1136. (c) Yoneda, N.; Nagata, S.; Fukuhara, T.; Suzuki, A. A melamine/HF-carbon tetrachloride liquid-liquid two-phase mixture. A highly versatile hydrofluorinating agent for alkenes to facilitate continuous operations. Chem. Lett. 1984, 13, 1241-1242. (d) Olah, G. A.; Li, X.-Y. Poly-4-vinylpyridinium Poly(hydrogen fluoride): A Convenient Polymeric Fluorinating Agent. Synlett 1990, 267-269. (e) Bucsi, I.; Török, B.; Marco, A. I.; Rasul, G.; Prakash, G. K. S.; Olah, G. A. Stable Dialkyl Ether/Poly(Hydrogen Fluoride Complexes: Ether/Poly(Hydrogen Fluoride), A New, Convenient, and Effective Fluorinating Agent. J. Am. Chem. Soc. 2002, 124, 7728-7736. (f) Hara, S.; Kameoka, M.; Yoneda, N. The 5 or 6 HF-Et₃N complex, mild, and selective hydrofluorination agents for tertalkyl fluorides Synlett 1996, 529-530. (g) Thibaudeau, S.; Martin-Mingot, A.; Jouannetaud, M. P.; Karam, O.; Zunino, F. A novel, facile route to β-fluoroamines by hydrofluorination using superacid HF-SbF₅. Chem. Commun. 2007, 30, 3198-3200. (h) Lu, Z.; Zeng, X.; Hammond, G. B.; Xu, B. Widely Applicable Hydrofluorination of Alkenes via Bifunctional Activation of Hydrogen Fluoride. J. Am. Chem. Soc. 2017, 139, 18202. (i) Lu, Z.; Bajwa, B. S.; Otome, O. E.; Hammond, G. B.; Xu, B. Multifaceted Ion Exchange Resin-Supported Hydrogen Fluoride: A Path to Flow Hydrofluorination. Green Chem. 2019, 21, 2224-2228.
- (11) Bertrand, X.; Paquin, J.-F. Direct Hydrofluorination of Methallyl Alkenes Using a Methanesulfonic Acid/Triethylamine Trihydrofluoride Combination. *Org. Lett.* **2019**, 21, 9759.
- (12) Wilger, D.; Grandjean, J.; Lammert, T.; Nicewicz, D. A. The direct anti-Markovnikov addition of mineral acids to styrenes. *Nat. Chem.* **2014**, *6*, 720–726.
- (13) Mandal, A.; Jang, J.; Yang, B.; Kim, H.; Shin, K. Palladium-Catalyzed electrooxidative hydrofluorination of aryl-substituted alkenes with a nucleophilic fluorine source. *Org. Lett.* **2023**, 25, 1, 195–199.
- (14) Hoogesteger, R.H.; Murdoch, N.; Cordes, D.B.; Johnston, C.P. Cobalt-Catalyzed Wagner-Meerwein Rearrangements with Concomitant Nucleophilic Hydrofluorination. *Angew. Chem., Int. Ed.* **2023**, e202308048.

- (15) HF (pKa=3.2 in H_2O) is substantially less acidic compared to carbocation (pKa=-3 in H_2O); thus, the direct protonation of alkene to generate carbocation is unfavorable.
- (16) Nakagawa, M.; Matsuki, Y.; Nagao, K.; Ohmiya, H. A Triple Photoredox/Cobalt/Brønsted Acid Catalysis Enabling Markovnikov Hydroalkoxylation of Unactivated Alkenes. *J. Am. Chem. Soc.* **2022**, 144, 7953–7959.
- (17) (a) Wu, X.; Gannett, C.N.; Liu, J.; Zeng, R.; Novaes, L.F.T.; Wang, H.; Abruña, H.D.; Lin, S. Intercepting Hydrogen Evolution with Hydrogen-Atom Transfer: Electron-Initiated Hydrofunctionalization of Alkenes. *J. Am. Chem. Soc.* **2022**, 144, 17783–17791. For a related work on electrocatalytic HAT via an oxidative mechanism, see: (b) Song, L.; Fu, N.; Ernst, B. G.; Lee, W. H.; Frederick, M. O.; DiStasio, R. A. Jr.; Lin, S. Dual Electrocatalysis Enables Enantioselective Hydrocyanation of Conjugated Alkenes. *Nat. Chem.* **2020**, *12*, 747–754.
- (18) Gnaim, S.; Bauer, A.; Zhang, H.-J.; Chen, L.; Gannett, C.; Malapit, C.A.; Hill, D.E.; Vogt, D.; Tang, T.; Daley, R.A.; Hao, W.; Zeng, R.; Quertenmont, M.; Beck, W.D.; Kandahari, E.; Vantourout, J. C.; Echeverria, P.-G.; Abruna, H.D.; Blackmond, D.G.; Minteer, S.D.; Reisman, S.E.; Sigman, M.S.; Baran, P.S. Cobaltelectrocatalytic HAT for functionalization of unsaturated C-C bonds. *Nature* **2022**, 605, 687–695.
- (19) (a) Sun, H.-L.; Yang, F.; Ye, W.-T.; Wang, J.-J.; Zhu, R. Dual Cobalt and Photoredox Catalysis Enabled Intermolecular Oxidative Hydrofunctionalization. *ACS Catal.* **2020**, 10, 4983–4989. (b) Yang, F.; Nie, Y.-C.; Liu, H.-Y.; Zhang, L.; Mo, F.; Zhu, R. Electrocatalytic Oxidative Hydrofunctionalization Reactions ofAlkenes via Co (II/III/IV) Cycle. *ACS Catal.* **2022**, 2132–2137. (20) (a) Park, S. H.; Jang, J.; Shin, K.; Kim, H. Electrocatalytic Radical-Polar Crossover Hydroetherification of Alkenes with Phenols. *ACS Catal.* **2022**, 12, 10572–10580. (b) Park, S. H.; Bae, G.; Choi, A.; Shin, S.; Shin, K.; Choi, C. H.; Kim, H. Electrocatalytic Access to Azetidines via Intramolecular Allylic Hydroamination: Scrutinizing Key Oxidation Steps through Electrochemical Kinetic Analysis. *J. Am. Chem. Soc.* **2023**, 145, 28, 15360–15369.
- (21) (a) Qin, T.; Lv, G.; Meng, Q.; Zhang, G.; Xiong, T.; Zhang, Q. Cobalt-Catalyzed Radical Hydroamination of Alkenes with N-Fluorobenzenesulfonimides. *Angew. Chem., Int. Ed.* **2021**, 60, 25949–25957. (b) Qin, T.; Lv, G.; Miao, H.; Guan, M.; Xu, C.; Zhang, G.; Xiong, T.; Zhang, Q. Cobalt-Catalyzed Asymmetric Alkylation of (Hetero)Arenes with Styrenes. *Angew. Chem., Int. Ed.* **2022**, 61, e202201967. (c) Miao,H.; Guan, M.; Xiong, T.; Zhang, G.; Zhang, Q. Cobalt-Catalyzed Enantioselective Hydroamination of ArylalkeneswithSecondaryAmines. *Angew. Chem., Int. Ed.* **2023**, 62, No. e202213913.
- (22) (a) Touney, E. E.; Foy, N. J.; Pronin, S. V. Catalytic Radical-Polar Crossover Reactions of Allylic Alcohols. *J. Am. Chem. Soc.* **2018**, 140, 16982–16987. (b) Discolo, C. A.; Touney, E. E.; Pronin, S. V. Catalytic Asymmetric Radical-Polar Crossover Hydroalkoxylation. *J. Am. Chem. Soc.* **2019**, 141, 17527–17532.
- (23) Wilson, C. V.; Kim, D.; Sharma, A.; Hooper, R. X.; Poli, R.; Hoffman, B. M.; Holland, P. L. Cobalt–Carbon Bonding in a Salen-Supported Cobalt(IV) Alkyl Complex Postulated in Oxidative MHAT Catalysis. *J. Am. Chem. Soc.* **2022**, 144, 10361–10367.
- (24) Ebisawa, K.; Izumi, K.; Ooka, Y.; Kato, H.; Kanazawa, S.; Komatsu, S.; Nishi, E.; Shigehisa, H. Catalyst- and Silane-Controlled Enantioselective Hydrofunctionalization of Alkenes by Cobalt-Catalyzed Hydrogen Atom Transfer and Radical-Polar Crossover. *J. Am. Chem. Soc.* **2020**, 142, 13481–13490.
- (25) Chou, T. S.; Becke, L. M.; O'Toole, J. C.; Carr, M. A.; Parker, B. E. Triethylamine poly(hydrogen fluorides) in the synthesis of a fluorinated nucleoside glycon. *Tetrahedron Lett.* **1996,** 37, 17–20.

- (26) (a) Topczewski, J. T.; Tewson, T. J.; Nguyen, H. M. Iridium-Catalyzed Allylic Fluorination of Trichloroacetimidates *J. Am. Chem. Soc.* **2011**, 133, 19318–19321. (b) Webb, E. W.; Park, J. B.; Cole, E. L.; Donnelly, D. J.; Bonacorsi, S. J.; Ewing, W. R.; Doyle, A. G. Nucleophilic (Radio)Fluorination of Redox-Active Esters Via Radical-Polar Crossover Enabled by Photoredox Catalysis. *J. Am. Chem. Soc.* **2020**, 142, 9493–9500. (c) Zhang, L.; Cheng, X.; Zhou, Q.-L. Electrochemical Synthesis of Sulfonyl Fluorides with Triethylamine Hydrofluoride. *Chin. J. Chem.* **2022**, 40, 1687–1692.
- (27) DiRocco, D. Electrochemical Series of Photocatalysts and Common Organic Compounds; Merck: 2014.
- (28) (a) Kaljurand, I.; Kutt, A.; Soovali, L.; Rodima, T.; Maemets, V.; Leito, I.; Koppel, I. A. Extension of the Self-Consistent Spectrophotometric Basicity Scale in Acetonitrile to a Full Span of 28 pKa Units: Unification of Different Basicity Scales. *J. Org. Chem.* **2005**, 70, 1019–1028. (b) Kütt, A.; Selberg, S.; Kaljurand, I.; Tshepelevitsh, S.; Heering, A.; Darnell, A.; Kaupmees, K.; Piirsalu, M.; Leito, I. pKa values in organic chemistry Making maximum use of the available data. *Tetrahedron Lett.* **2018**, 59, 3738–3748. (c) Elgrishi, N.; Kurtz, D. A.; Dempsey, J. L. Reaction Parameters Influencing Cobalt Hydride Formation Kinetics: Implications for Benchmarking H₂-Evolution Catalysts. *J. Am. Chem. Soc.* **2017**, 139, 239–244.
- (29) Pearson, R. M.; Lim, C.-H.; McCarthy, B. G.; Musgrave, C. B.; Miyake, G. M. Organocatalyzed Atom Transfer Radical Polymerization Using N-Aryl Phenoxazines as Photoredox Catalysts. *J. Am. Chem. Soc.* **2016**, 138, 11399–11407.
- (30) Excited 4CzIPN **2** is not reducing enough ($E_{1/2}$ [2^*]/ [2^*] = -1.18 V vs SCE) to reduce Co^{II} to Co^{I} . For **3**, E^{0^*} ([PC^{**}]/[$^{3}PC^{*}$] = 1.93V vs. SCE), it is likely that higher loading of the photocatalyst is required. Organ photocatalysts usually have a shorter-lived excited triplet state compared to iridium-based photocatalyst, which might explain why SET is not efficient. It could also be that the radical cation is less oxidizing compared to Ir IV ($E_{1/2}$ [Ir^{IV}]/[Ir^{III}] = 0.77 V vs SCE), it's been reported to be E^{0} ([3^{**}]/[3] = 0.48 V vs. SCE) (see ref 27). This potential should be able to oxidize the radical species or Co^{III} -alkyl; however, kinetically, it might be slower compared to Ir^{IV} .
- (31) Watanabe, M.; Koike, H.; Ishiba, T.; Okada, T.; Seo, S.; Hirai, K. Synthesis and Biological Activity of Methanesulfonamide Pyrimidine- and N-Methanesulfonyl Pyrrole-Substituted 3,5-Dihydroxy-6-Heptenoates, a Novel Series of HMG-CoA Reductase Inhibitors. *Bioorg. Med. Chem.* **1997**, 5, 437–444.
- (32) (a) Wayner, D. D. M.; McPhee, D. J.; Griller, D. Oxidation and Reduction Potentials of Transient Free Radicals. *J. Am. Chem. Soc.* **1988**, 110, 132. (b) Wayner, D. D. M.; Houmam, A. Redox Properties of Free Radicals. *Acta Chem. Scand.* **1998**, 52, 377.
- (33) Boucher, D.G., Pendergast, A.D., Wu, X., Nguyen, Z.A., Jadhav, R.G., Lin, S., White, H.S. and Minteer, S.D. Unraveling Hydrogen Atom Transfer Mechanisms with Voltammetry: Oxidative Formation and Reactivity of Cobalt Hydride. *J. Am. Chem. Soc.* **2023**. 145, 17665-17677.
- (34) (a) Crossley, S. W.; Barabe, F.; Shenvi, R. A. Simple, chemoselective, catalytic olefin isomerization. *J. Am. Chem. Soc.* **2014**, 136(48), 16788–91. (b) Halpern, J. Determination and Significance of Transition-Metal Alkyl Bond Dissociation Energies. *Acc. Chem. Res.* **1982**, 15(8), 238–244. (c) Chiang, L.; Allan, L. E. N.; Alcantara, J.; Wang, M. C. P.; Storr, T.; Shaver, M. P. *Dalton Trans.* **2014**, 43, 4295. (d) Demarteau, J.; Debuigne, A.; Detrembleur, C. Organocobalt Complexes as Sources of Carbon-Centered Radicals for Organic and Polymer Chemistries. *Chem. Rev.* 2019, 119, 6906–6955.

- (35) $E_{1/2}$ (Fc/Fc⁺) = +0.450 V vs. SCE in DMF with Bu₄NPF₆ as electrolyte. Connelly, N. G.; Geiger, W. E. Chemical redox agents for organometallic chemistry. *Chem. Rev.* **1996**, 96, 877–910. (36)(a) Artero, V.; Fontecave, M. Some general principles for designing electrocatalysts with hydrogenase activity. *Coord. Chem. Rev.* **2005**, 249, 1518–1535. (b) Hu, X.; Brunschwig, B. S.; Peters, J. C. Electrocatalytic hydrogen evolution at low overpotentials by cobalt macrocyclic glyoxime and tetraimine complexes. *J. Am. Chem. Soc.* **2007**, 129, 8988–8998. (c) Baffert, C.; Artero, V.; Fontecave, M. Cobaloximes as functional models for hydrogenases. 2. Proton electroreduction catalyzed by difluoroborylbis(dimethylglyoximato)-cobalt(II)complexes in organic media. *Inorg. Chem.* **2007**, 46, 1817–1824.
- (37) It has been previously shown that Co^{III}-alkyl species with salen-type ligands are reduced at around -2.2 V vs Fc/Fc⁺. See: Zubaydi, S.; Onuigbo, I.; Truesdell, B.; Sevov, C. Cobalt-Catalyzed Electroreductive Alkylation of Unactivated Alkyl Chlorides with Conjugated Olefins. *Angew. Chem. Int. Ed.* **2023**, e202313830.
- (38) In our previous publication (see ref 17 SI), we concluded on the basis of voltammetry data and simulation that Co^{III}-alkyl with a salen ligand can be reduced to Co^{II}-alkyl under a similar potential at which the free Co^{III} catalysts is reduced to Co^{II} state. However, based on recent literature data from ref 37, this is likely an inaccurate hypothesis.
- (39) (a) Zhao, Y.; Truhlar, D. G. A new local density functional for main-group thermochemistry, transition metal bonding, thermochemical kinetics, and noncovalent interactions. *J. Chem. Phys.* **2006**, 125, 194101. (b) Weigend, F.; Ahlrichs, R. Balanced Basis Sets of Split Valence, Triple Zeta Valence and Quadruple Zeta Valence Quality for H to Rn: Design and Assessment of Accuracy. *Phys. Chem. Chem. Phys.* **2005**, 7, 3297–3305. (c) Weigend, F. Accurate Coulomb-fitting basis sets for H to Rn. *Phys. Chem. Chem. Phys.* **2006**, 8, 1057–1065. (d) Marenich, A. V.; Cramer, C. J.; Truhlar, D. G. Universal Solvation Model Based on Solute Electron Density and on a Continuum Model of the Solvent Defined by the Bulk Dielectric Constant and Atomic Surface Tensions. *J. Phys. Chem. B* **2009**, 113, 6378–6396.
- (40) This competition behavior has also been observed using differential electrochemical mass spectrometry. See ref 17 for details.
- (41) We note that the energies of charged species such as carbocations are difficult to accurately estimate even when using solvation models, but that these calculations presented here provide a semi-quantitative estimation of the equilibrium trend in these chemical events.
- (42) The fluoride trapping of carbocation (III) was assumed to be under diffusion control according to Mayr's equation. The first-order rate constant for the diffusion-limited ion combination is ca. 10^{10} M⁻¹ s⁻¹ × 1 M (the concentration of fluoride), which corresponds to an effective activation free energy of ca. 3.8 kcal/mol. For more discussion on diffusion-controlled reactions, see: (a) Mayr, H.; Ofial, A. R. Kinetics of Electrophile-Nucleophile Combinations: A General Approach to Polar Organic Reactivity Pure Appl. Chem. 2005, 77, 1807-1821. (b) Nolte, C.; Ammer, J.; Mayr, H. Nucleofugality and Nucleophilicity of Fluoride in Protic Solvents. J. Org. Chem. 2012, 77, 3325-3335. (c) Limanto, J.; Tallarico, J. A.; Porter, J. R.; Khuong, K. S.; Houk, K. N.; Snapper, M. L. Intramolecular Cycloadditions of Cyclobutadiene with Olefins. J. Am. Chem. Soc. 2002, 124, 14748-14758. (d) Wang, Y.; Yu, Z.-X. Intra- versus Intermolecular Carbon-to-Carbon Proton Transfers in the Reactions of Arynes with Nitrogen Nucleophiles: A DFT Study. J. Org. Chem. 2018, 83, 5384-5391.

(43) However, at this stage we are unable to conclusively rule out pathway ${\bf a}$ as it remains possible, although unlikely, that radical (I) undergoes facile oxidation to form carbocation (III) prior to reacting with Co^{II} to form intermediate (II), and carbocation (III) then undergoes reaction with F- directly before

reacting with Co^{II} to form adduct (IV). Without knowing the relative rate of (I) undergoing oxidation vs. recombination with Co^{II} , or the relative rate of (III) reacting with F- vs. Co^{II} , we cannot draw a definitive conclusion here.

Insert Table of Contents artwork here